Highly luminescent metallacages featuring bispyridyl ligands functionalised with BODIPY for imaging in cancer cells

Ben Woods,†[a] Daniel Döllerer,†[a,b] Brech Aikman,[a] Margot Wenzel,[a] Edward J. Sayers,[c] Fritz. E. Kühn,[b] Arwyn T. Jones,[c] and Angela Casini *[a]

a. School of Chemistry, Cardiff University, Park Place, CF10 3AT Cardiff, Wales, United Kingdom.

b. Molecular Catalysis, Department of Chemistry, Catalysis Research Center, Technische Universität München, Lichtenbergstr. 4, 85747 Garching bei München, Germany.

c. School of Pharmacy and Pharmaceutical Sciences, Cardiff University, CF10 3NB Cardiff, Wales, United Kingdom.

† co-first authorship.

Email corresponding author: CasiniA@cardiff.ac.uk; Ph: +44 29 2087 6364.

Abstract. Recently, 3-dimensional supramolecular coordination complexes of the metallacage type have been shown to hold promise as drug delivery systems for different cytotoxic agents, including the anticancer drug cisplatin. However, so far only limited information is available on their uptake and sub-cellular localisation in cancer cells. With the aim of understanding the fate of metallacages in cells by fluorescence microscopy, three fluorescent Pd_2L_4 metallacages were designed and synthesised by self-assembly of two types of bispyridyl ligands (L), *exo*-functionalised with boron dipyrromethene (BODIPY) moieties, with Pd(II) ions. The cages show high quantum yields and are moderately stable in the presence of physiologically relevant concentration of glutathione. Furthermore, the cages are able to encapsulate the anticancer drug cisplatin, as demonstrated by NMR spectroscopy. Preliminary cytotoxicity studies in a small panel of human cancer cells showed that the metallacages are scarcely toxic *in vitro*. The marked fluorescence due to BODIPY allowed us to visualise the

cages' uptake and sub-cellular localisation inside melanoma cells using fluorescence microscopy, highlighting uptake *via* active transport mechanisms and accumulation in cytoplasmic vesicles.

Keywords: supramolecular coordination complexes; metallacages; cisplatin; fluorescence microscopy; cancer.

Introduction

Supramolecular coordination complexes (SCCs) have been attracting increasing attention over the past few decades due to their several potential applications in different areas, including sensing, molecular recognition and catalysis.[1] More recently, SCCs have been designed for biomedical applications, including as anticancer drugs or as novel drug delivery systems.[2,3] The latter application still needs validation, but the high versatility of these supramolecular systems holds great promise. Overall, SCCs as drug delivery systems can be based on *i)* both encapsulation of a drug, driven by hydrophobic interactions between the cargo drug molecule and the host cavity, and non-covalent interactions within the host cavity, as well as *ii)* covalent bonding of a *prodrug* species to the SCC architecture.[2]

In this context, inspired by the work of Therrien,[4,5] Crowley[6] and others,[2,7] we have explored the potential of metallacages - of the Pd_2L_4 type (L = 3,5-bis(3-ethynylpyridine)phenyl) - as novel drug delivery systems for the anticancer drug cisplatin.[8] Thus, we exploited the host-guest properties of the cages to encapsulate cisplatin and protect it from speciation. NMR spectroscopy and X-ray diffraction studies showed encapsulation of two cisplatin molecules per cage unit.[8] Of note, the selected metallacages are non-toxic in both cells and tissues, making them suitable for application as drug delivery vectors.[8]

More recently, we developed a method to bioconjugate Pd_2L_4 cages to peptides based on amide bond formation between the cage-ligands and amino or carboxylic acid groups in the peptide chain.[9] Thus, we selected peptidic ligands for targeting of integrins overexpressed in cancer cells.[10] The results showed that cisplatin encapsulated in the targeted cages had a two-fold increase in cytotoxic potency in melanoma cells after 24 h incubation.[10] Moreover, reduced toxicity of cisplatin encapsulated in integrin-targeted metallacages was also demonstrated in healthy tissues *ex vivo*.[10]

While the Pd_2L_4 cages are very promising for cisplatin delivery, their mechanism of cancer cell uptake is still not fully understood; this prevents their optimisation as targeted drug vectors. In order to

study the cages intracellular accumulation and sub-cellular localisation, fluorescence microscopy is the preferred technique, allowing analysis with intact cells while avoiding complex cell fractionation steps which may lead to reduced analyte recovery, and lack of reproducibility.

Although the ligands used to build the cages are highly luminescent, upon self-assembly quenching of their fluorescence is normally observed due to the so-called 'heavy metal' effect.[8] While the emissive properties of metallacages have been discussed,[11,12] examples of highly emissive Pd_2L_4 cages are rare. Previously, we have reported on a number of Pd_2L_4 cages *exo*-functionalised with luminescent moieties, including anthracenyl groups[13] and Ru(II) polypyridyl ligands.[14] However, while the former did not display sufficient luminescence due to the lowered probability of π-π* excitation upon conjugation of the fluorophore to the ligand scaffold,[13] the latter achieved strong emission only upon excitation in the UV region,[14] which is not ideal for conventional microscopy analysis.

Here, we developed a new family of Pd_2L_4 cages *exo*-functionalised with highly fluorescent boron dipyrromethene (BODIPY) scaffolds. BODIPYs are a family of fluorescent dyes used for many applications such as solar cells,[15] imaging[16] and photodynamic therapy.[17] The characteristic fluorescence of the BODIPY moieties conjugated to the metallacages enables their intracellular visualisation using fluorescence microscopy. Other supramolecular structures, such as Ru(II) metalla-rectangles, containing BODIPY ligands have been reported, but these were used as cytotoxic agent *per se* and not as drug delivery systems.[18,19]

Three new BODIPY-cages, featuring either an amide bond or a 1,2,3-triazole ring to tether the cage bispyridyl scaffold to the fluorophore, were synthesised by self-assembly and characterised by various methods, including NMR spectroscopy, high-resolution mass spectrometry and fluorescence spectroscopy. Furthermore, the stability of the cages in aqueous solution was investigated using UV-Visible spectroscopy, while their interactions with physiologically relevant concentrations of glutathione (GSH), which is a common intracellular antioxidant with an increased level in cancer cells, were investigated by ^{1}H NMR spectroscopy. The encapsulation of cisplatin was also studied by both ^{1}H and ^{195}Pt NMR spectroscopy. The antiproliferative effects of the cages were assessed in the human malignant melanoma A375 cell line to evaluate possible cytotoxic effects, while the uptake and sub-cellular distribution of selected metallacages were studied by fluorescence wide-field and confocal microscopy.

Results and discussion

Synthesis

The synthesis of highly luminescent Pd_2L_4 metallacages was achieved by the conjugation of the BODIPY fluorophore to the bispyridyl ligand scaffold. This could be formed either *via* amide bond formation or by copper catalysed azide-alkynyl cycloaddition (CuAAC) reaction depending on the functional groups of the fluorophore and ligand. Thus, an amine *exo*-functionalised ligand was synthesised *via* Sonogashira cross coupling between dibromoaniline and two equivalents of 3-ethynyl pyridine, according to a previously reported procedure,[14] to afford the amine functionalised ligand (**L1**). Afterwards, **L1** could be converted to the corresponding azide *exo*-functionalised ligand by *in situ* substitution of the amine for a reactive nitro group, followed by substitution of the nitro group to afford the corresponding azide functionalised ligand (**L2**) (Scheme S1).

The BODIPY fluorophores were synthesised by adapting previously reported procedures.[20–22] In details, 3-ethyl-2,4-methylpyrrole was stirred at room temperature in dichloromethane (DCM) with the appropriate *para*-functionalised benzaldehyde in the presence of catalytic amounts of trifluoroacetic acid (TFA) to afford the organic scaffold of the BODIPY fluorophore. The functional group of the final BODIPY could be easily modified by the choice of the *para*- functional group of the benzaldehyde starting material. Coordination of the BF_2 moiety to the organic scaffold was accomplished by first deprotonating the pyrrole functional groups using 2,3-dichloro-5,6-dicyano-1,4-benzoquinone (DDQ), before introducing boron trifluoride diethyl etherate in the presence of triethylamine to produce the carboxylic acid functionalised BODIPY (**B1**) and alkynyl functionalised BODIPY (**B2**).

L1 was coupled to **B1** *via* classical amide bond formation to afford **LB1** (Scheme S2). **L1, B1,** 1-chloro-2-methylpyridinium iodide (CMPI), and 4-dimethylaminopyridine (DMAP) were stirred in dimethylformamide (DMF) at 130 °C for 16h, before purification *via* chromatography on silica to give BODIPY functionalised ligand **LB1**. **L2** was coupled to **B2** *via* CuAAC “click” chemistry to achieve **LB2** (Scheme S3). In detail, **L2** and **B2** were dissolved in DCM and the solution diluted with a solution of methanol:water (3:1). The reducing agent, sodium ascorbate, was made *in situ* by dissolving *L*-(+)-ascorbic acid with sodium hydroxide in water. To this mixture, $CuSO_4$ was added and the resulting aqueous solution was added to the organic solution containing **L2** and **B2** and stirred at room

temperature for 5 h. The reaction was quenched using ammonium acetate, before the solution was extracted with DCM and purified *via* chromatography on silica to afford the BODIPY functionalised ligand **LB2**.

Finally, the BODIPY *exo*-functionalised Pd_2L_4 metallacages were formed *via* self-assembly by mixing 4 equiv. of ligand **LB1** or **LB2** with 2 equiv. of Pd^{2+} at room temperature in DMSO to afford cage **C1.X** (X = BF_4^-, NO_3^-) or **C2.NO$_3$**, respectively (Scheme 1). The counterion could be varied using the appropriate Pd^{2+} salt (see supplementary material for details). All the ligand precursors and cages were characterised by various methods, including ^{1}H, ^{13}C, ^{11}B and ^{19}F NMR spectroscopy and high-resolution mass spectrometry. The obtained results indicate that discreet supramolecular complexes of the formula Pd_2L_4 form *via* self-assembly under these conditions. Representative ^{1}H NMR spectra for ligand **LB1** and cage are compared in Figure 1 and show that, upon cage formation, significant downfield chemical shifts of protons peaks H_a and H_b, indicative of coordination to the Pd(II) ions, can be observed in accordance with previously reported studies.[8,10,11] Furthermore, the ligands and cages were studied for their emission properties, and the respective quantum yields (Table 1) calculated as described in the experimental section. Of note, at variance with previously reported metallacages *exo*-functionalised with different fluorophores,[13] the BODIPY-cages maintained excellent quantum yield values. Of note, the BODIPY-cages have been designed with a scaffold featuring slightly longer 'linkers' between the fluorogenic moiety and the ligand L with respect to previously reported cages,[13] which may reduce the conjugation between the two systems preventing the quenching of the fluorescence upon self-assembly.

UV-Visible spectrophotometry stability studies

The stability of the metallacages **C1.BF$_4$**, **C1.NO$_3$**, and **C2.NO$_3$** in water and phosphate buffered saline (PBS, pH 7.4) was studied by UV-Visible spectrophotometry. As shown in Figures S22-S24, the absorption spectra of the three cages, featuring two main bands at ca. 300 and 530 nm, were completely stable in water over 24 h. Metallacages **C1.BF$_4$** and **C1.NO$_3$** were also sufficiently stable in PBS solution (pH 7.4) although marked reduction of the two absorption bands was observed at 4 h incubation and continued over the 24 h period. While over 24 h a precipitate was formed in solution, shaking of the cuvette partly restored the original absorption spectrum (see Fig. S22-S23). It should be noted that the solubility of metallacages is determined by a number of factors, including the

properties of the main ligand scaffolds, the metal ion, as well as the type of counter ion balancing the cage overall positive charge. In such a complex interplay of elements it is difficult to establish what causes cage precipitation and/or instability in solution. Furthermore, it should be noted that the BODIPY-ligand system also presents some issues of solubility/stability in buffered solution, most probably due to the hydrolysis of the B-F moiety. Certainly, from the obtained UV-visible data, the presence of other anions in the buffer (pH 7.4) favours the observed spectra changes, and formation of a precipitate in solution.

The spectrum of metallacage **C2.NO$_3$** in PBS solution underwent even more pronounced reduction of intensity after only 2 h (Figure S24), and any attempt to re-dissolve the precipitate would not restore the original signal intensity. Therefore, Pd_2L_4 metallacage **C2.NO$_3$** was not used for further biological characterisation due to its poor solubility in physiological media. The enhanced instability of the **C2.NO$_3$** cage with respect to the BF_4^- derivatives may be attributed to possible increased encapsulation of the nitrate ion into the cavity, as well as to its higher coordinating affinity towards the Pd(II) centres.

Interactions with GSH

Afterwards, we examined the stability of the cages in the presence of physiologically relevant concentration of glutathione (GSH, 2 mM) by NMR spectroscopy. Therefore, GSH was added to a solution of cage **C1.BF$_4$** in DMSO-d_6:D_2O (9:1) and ^{1}H NMR spectra were recorded over time over 18 h (Figure 2). The obtained results show that, upon addition of GSH, the metallacage disassembles into its precursors, as shown by the appearance of the peaks characteristic of the ligand **LB1**. However, part of the cage remains stable over time (ca. 30%, calculated by comparing the integral value of peak H_b of the metallacage to the peak of H_b of the ligand), and only further addition of excess GSH allows complete disintegration of **C1.BF$_4$** (Figure 2). This observation supports the hypothesis that the cage can partly remain intact in the cytosol.

Encapsulation of cisplatin

^{1}H NMR spectroscopy

We have previously demonstrated the encapsulation of cisplatin within Pd_2L_4 metallacages *via* ^{1}H NMR spectroscopy in DMF-d_7.[10,23] Similarly, metallacages **C1.BF$_4$** and **C1.NO$_3$** were dissolved in DMF-d_7 and the respective ^{1}H NMR spectra were recorded. Afterward, two equiv. of cisplatin were added to

the deuterated solution and a second ^{1}H NMR spectrum was recorded and compared with the previous one. The chemical shifts of all the proton signals were then compared between the spectra of **C1.BF$_4$** and encapsulated (cisplatin)$_2$⊂**C1.BF$_4$** (Figure S25) and between **C1.NO$_3$** and (cisplatin)$_2$⊂**C1.NO$_3$** (Figure S26). In both cases, the same three proton signals - namely, the two signals corresponding to the protons facing the internal cavity (H_a and H_e), as well as the signal of the *exo*-facing proton (H_b), which is alpha to the coordinating nitrogen of the ligand - were observed to undergo chemical shifts changes due to cisplatin encapsulation, as previously reported.[23]

Specifically, the signals of the cavity facing protons, H_a and H_e, for (cisplatin)$_2$⊂**C1.BF$_4$** both underwent a slight downfield shift (+0.03 ppm and +0.08 ppm, respectively) when compared to **C1.BF$_4$** (Figure S25). Furthermore, for both cages, the signal of the central cavity facing proton, H_e, was significantly broadened, suggesting intermolecular interactions between the host Pd_2L_4 metallacage and the cisplatin guest molecule.

However, upon comparison of the ^{1}H NMR spectra of (cisplatin)$_2$⊂**C1.NO$_3$** and **C1.NO$_3$**, the cavity facing proton (H_a and H_e) signals undergo a very small upfield shift (-0.02 ppm in both cases). We have previously reported a similar observation between Pd_2L_4 type metallacages which differ only in their counterions (either NO_3^- or BF_4^-).[23] This finding are in line with previous studies by Crowley and co-workers,[24] according to which while the NO_3^- counterion can be encapsulated within the Pd_2L_4 metallacage, BF_4^- is not. Therefore, the cavity facing protons of **C1.NO$_3$** are in close proximity to the negatively charged NO_3^-, and thus, their signals are shifted further downfield compared to **C1.BF$_4$**, in which the cavity is occupied by neutral solvent molecules. Upon encapsulation of cisplatin to **C1.NO$_3$**, the counterion is exchanged for cisplatin as the guest and the signals of the cavity facing protons undergo a slight upfield shift. In the case of **C1.BF$_4$**, the counterion is not encapsulated within the cavity, and so the downfield shift of the signals of the cavity facing protons can be attributed to the evacuation of solvent molecules, and the occupation of the cavity with cisplatin.

^{195}Pt NMR spectroscopy

In order to further characterise the encapsulation of cisplatin within the metallacage **C1.BF$_4$**, ^{195}Pt NMR spectroscopy was applied. Initially, one equiv. of cisplatin was dissolved in DMF (0.5 mL) and this solution was added to the NMR tube with a capillary insert filled with DMF-d_7 and a spectrum was recorded (Figure 3, top spectrum). To this solution, one equiv. of metallacage was added and a second

^{195}Pt spectrum was recorded in order to obtain a 1:1 cisplatin:cage stoichiometry (Figure 3, bottom spectrum). Finally, a second equiv. of cisplatin was added to the metallacage containing solution and a third spectrum was recorded (Figure 3, middle spectrum). Comparison of the spectra showed that upon addition of metallacage **C1.BF$_4$** an upfield shift (δ [ppm] = -1.9) was observed for the ^{195}Pt peak of cisplatin at -2080.2 ppm. This shift is indicative of the fact that the ^{195}Pt nucleus is experiencing more electronic shielding due to encapsulation within the metallacage cavity. The shift is fully resolved for the sample containing two equiv. of cisplatin, in accordance with previously reported studies.[23]

Antiproliferative effects

The antiproliferative effects of cisplatin encapsulated in cage **C1.BF$_4$** were studied against the human malignant melanoma A375 cell line after 24 h incubation, when the free metallodrug is known to be poorly active. This also allowed for microscopy analysis at suitable metallodrug concentration levels (see Experimental for details). The resulting EC_{50} (concentration of a drug that gives half-maximal response) values are reported in Table 2 and show that the cage and respective ligand precursor are non-toxic at the highest tested concentration (EC_{50} > 50 μM). We also repeated the study with encapsulated cisplatin [(cisplatin)$_2$⊂**C1.BF$_4$**]. As these cage systems are not specifically targeted to human cancer cells, we did not expect to observe the same increase in the anticancer potency of cisplatin as observed for the previously published integrin-targeted metallacages.[10] In fact, the encapsulated cisplatin did not show any significant variation of the antiproliferative activity with respect to free cisplatin (Table 2).

Uptake and cellular localisation studies

The detection of the BODIPY-cages **C1.BF$_4$** and **C1.NO$_3$** and their respective ligand precursor **LB1** was achieved by fluorescence microscopy. The cages/ligand (5 μM) were incubated with A375 cells for 2 h at 37 °C, fixed and visualised by confocal fluorescence microscopy. **LB1** alone was observed in punctate structures and as diffuse labelling (Figure 4). Both cages **C1.NO$_3$** and **C1.BF$_4$** were internalised independently of the respective counter ions, to again label vesicular structures that were particularly prominent for **C1.BF$_4$**, with **C1.NO$_3$** enriched in a juxtanuclear region. Z-section analysis of cell treated with **C1.BF$_4$** confirmed the intracellular location of these compounds as opposed to aggregation and accumulation on the cell surface (Figure S27A). The results also show that the cage does not reach the cell nuclei to any significant extent.

Similar fluorescence profiles were observed in **LB1** and **B1** incubated cells (Figures 4 and S27B). Currently, it is impossible to determine if the cages remain intact or are disintegrated once internalised. The specific sub-cellular distribution observed for these particular BODIPY-cages is unexpected as other studies with BODIPY-containing metal-based scaffolds showed that they internalise into more non-descript diffuse structures,[25] rather than selectively accumulating in vesicles as particularly observed for **C1.BF$_4$**.

Finally, in order to establish if the mechanisms of cage uptake in cancer cells is active or relies on passive diffusion, we performed the same experiments at either 37 or 4 °C. The results are shown in Figure S28 and demonstrate that no fluorescence signal can be detected in cells incubated at 4 °C, thus, excluding passive, energy independent diffusion of the cages (and ligand) through the plasma membrane and pointing towards endocytosis as the mechanism of uptake.

Conclusions

We have reported here on the synthesis and characterisation of three new Pd_2L_4 metallacages featuring 3,5-bis(3-ethynylpyridine)phenyl ligands *exo*-functionalised with BODIPY units. The cages showed remarkable luminescent properties with quantum yields of 50-70% and excitation wavelength in the visible region (ca. 540 nm), which make them suitable for imaging in cells. The cages were studied for their stability in aqueous solution by UV-visible spectroscopy, and for their reactivity in the presence of physiologically relevant concentration of GSH. Of note, cage **C1.NO$_3$** dissociated only partially in the presence of this intracellular nucleophile. Moreover, the encapsulation properties of the anticancer drug cisplatin in the metallacages were studied by ^{1}H and ^{195}Pt NMR spectroscopy. The obtained results showed that up to 2 equiv. of cisplatin can be encapsulated in a cage molecule. The two cages in which the BODIPY moiety is linked to the cage scaffold by amide bond (**C1.BF$_4$** and **C1.NO$_3$**) were then tested against human A375 cancer cells showing no cytotoxic effects, which make them suitable for applications as drug delivery systems.

Moreover, the uptake and sub-cellular localisation of the cages in cancer cells was observed by both wide field and confocal fluorescence microscopy, revealing that cages are subjected to active endocytic transport, prior to accumulation in intracellular vesicles.

In future studies, it will be particularly interesting to identify the nature of the **C1.BF$_4$** labelled structures to determine if they are early endosomes, late endosomes/lysosomes or other structures such as melanosomes.

It will also be important to determine how this localisation of the cage affects the cisplatin release profile. Furthermore, preliminary Isothermal Titration calorimetry (ITC) data also show that cisplatin can be encapsulated in Pd_2L_4 metallacages in aqueous solution and in physiologically relevant concentrations. However, further studies are necessary to exclude cisplatin release prior uptake of the host-guest system.

Conflicts of interest

"There are no conflicts to declare".

Acknowledgements

A.C. acknowledges support from Cardiff University and the Hans Fischer Senior Fellowship of the Technical University of Munich – Institute for Advanced Study, funded by the German Excellence Initiative and the European Union Seventh Framework Program, under grant agreement n° 291763.

References

[1] A. Schmidt, A. Casini, F.E. Kühn, Coord. Chem. Rev. 275 (2014) 19–36. doi:10.1016/j.ccr.2014.03.037.

[2] A. Casini, B. Woods, M. Wenzel, Inorg. Chem. 56 (2017) 14715–14729. doi:10.1021/acs.inorgchem.7b02599.

[3] T.R. Cook, V. Vajpayee, M.H. Lee, P.J. Stang, K.W. Chi, Acc. Chem. Res. 46 (2013) 2464–2474. doi:10.1021/ar400010v.

[4] B. Therrien, Top Curr Chem. 319 (2012) 35–55. doi:10.1007/128.

[5] F. Schmitt, J. Freudenreich, N.P.E. Barry, L. Juillerat-Jeanneret, G. Süss-Fink, B. Therrien, J. Am. Chem. Soc. 134 (2012) 754–757. doi:10.1021/ja207784t.

[6] J.E.M. Lewis, E.L. Gavey, S.A. Cameron, J.D. Crowley, Chem. Sci. 3 (2012) 778–784. doi:10.1039/c2sc00899h.

[7] Y. R. Zheng, K. Suntharalingam, T. Johnstone, S. Lippard, Chem. Sci. 6 (2015) 1189–1193. doi:10.1038/nature13314.A.

[8] A. Schmidt, V. Molano, M. Hollering, A. Pöthig, A. Casini, F.E. Kühn, Chem. - A Eur. J. 22 (2016) 2253–2256. doi:10.1002/chem.201504930.

[9] J. Han, A. Schmidt, T. Zhang, H. Permentier, G.M.M. Groothuis, R. Bischoff, F.E. Kühn, P. Horvatovich, A. Casini, Chem. Commun. 53 (2017) 1405–1408. doi:10.1039/c6cc08937b.

[10] J. Han, A. Rader, F. Reichart, B. Aikman, M.N. Wenzel, B. Woods, M. Weinmüller, B.S. Ludwig, S. Sturup, G.M.M. Groothuis, H.P. Permentier, R. Bischoff, H. Kessler, P. Horvatovich, A. Casini, Bioconjug. Chem. (2018) acs.bioconjchem.8b00682. doi:10.1021/acs.bioconjchem.8b00682.

[11] J.E.M. Lewis, A.B.S. Elliott, C.J. McAdam, K.C. Gordon, J.D. Crowley, Chem. Sci. 5 (2014) 1833–1843. doi:10.1039/C4SC00434E.

[12] A.M. Johnson, O. Moshe, A.S. Gamboa, B.W. Langloss, J.F.K. Limtiaco, C.K. Larive, R.J. Hooley, Inorg. Chem. 50 (2011) 9430–9442. doi:10.1021/ic201092s.

[13] A. Schmidt, M. Hollering, M. Drees, A. Casini, F.E. Kühn, Dalton Trans. 45 (2016) 8556–8565. doi:10.1039/C6DT00654J.

[14] A. Schmidt, M. Hollering, J. Han, A. Casini, F.E. Kühn, Dalton Trans. 45 (2016) 12297–12300. doi:10.1039/c6dt02708c.

[15] T. Rousseau, A. Cravino, T. Bura, G. Ulrich, R. Ziessel, J. Roncali, Chem. Commun. (2009) 1673–1675. doi:10.1039/b822770e.

[16] T. Terai, T. Nagano, J. Physiol. 465 (2013) 347–359. doi:10.1007/s00424-013-1234-z.

[17] A. Kamkaew, S.H. Lim, H.B. Lee, L.V. Kiew, L.Y. Chung, K. Burgess, Chem. Soc. Rev. 42 (2013) 77–88. doi:10.1039/c2cs35216h.

[18] G. Gupta, A. Das, N.B. Ghate, T. Kim, J.Y. Ryu, J. Lee, N. Mandal, C.Y. Lee, Chem. Commun. 52 (2016) 4274–4277. doi:10.1039/c6cc00046k.

[19] G. Gupta, A. Das, K.C. Park, A. Tron, H. Kim, J. Mun, N. Mandal, K.W. Chi, C.Y. Lee, Inorg. Chem. 56 (2017) 4615–4621. doi:10.1021/acs.inorgchem.7b00260.

[20] M. Tomasulo, E. Deniz, R.J. Alvarado, F.M. Raymo, J. Phys. Chem. C. 112 (2008) 8038–8045. doi:10.1021/jp8009035.

[21] N.W. Smith, A. Alonso, C.M. Brown, S. V. Dzyuba, Biochem. Biophys. Res. Commun. 391 (2010) 1455–1458. doi:10.1016/j.bbrc.2009.12.091.

[22] B. Brizet, C. Bernhard, Y. Volkova, Y. Rousselin, P.D. Harvey, C. Goze, F. Denat, Org. Biomol. Chem. 11 (2013) 7729–7737. doi:10.1039/c3ob41370e.

[23] B. Woods, M.N. Wenzel, T. Williams, S.R. Thomas, R.L. Jenkins, A. Casini, Front. Chem. 7 (2019) 1–6. doi:10.3389/fchem.2019.00068.

[24] J.E.M. Lewis, J.D. Crowley, Supramol. Chem. 26 (2014) 173–181. doi:10.1080/10610278.2013.842644.

[25] S. Tasan, O. Zava, B. Bertrand, C. Bernhard, C. Goze, M. Picquet, P. Le Gendre, P. Harvey, F. Denat, A. Casini, E. Bodio, J. Chem. Soc. Dalt. Trans. 42 (2013) 6102–6109. doi:10.1039/c2dt32055j.

Figures and Tables

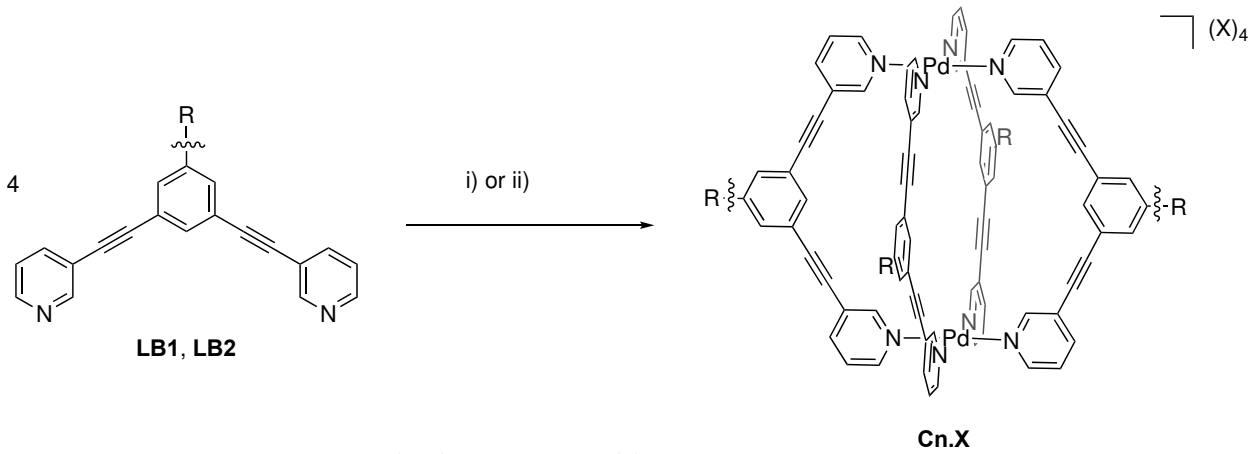

i) = 2([$Pd(CH_3CN)_4$](BF_4)$_2$), DMSO, r.t., 1 h

ii) = 2($Pd(NO_3)_2$), DMSO, r.t., 1 h

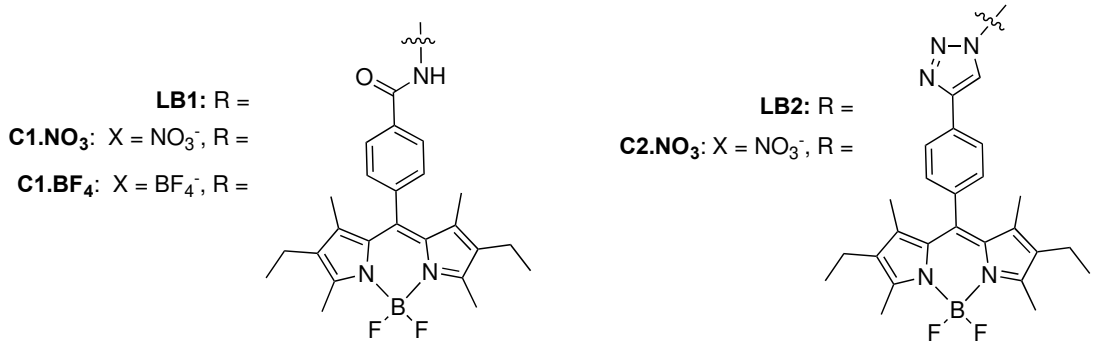

Scheme 1 - Synthesis of the Pd_2L_4 metallacages *exo*-functionalised with BODIPY fluorophores reported in this study.

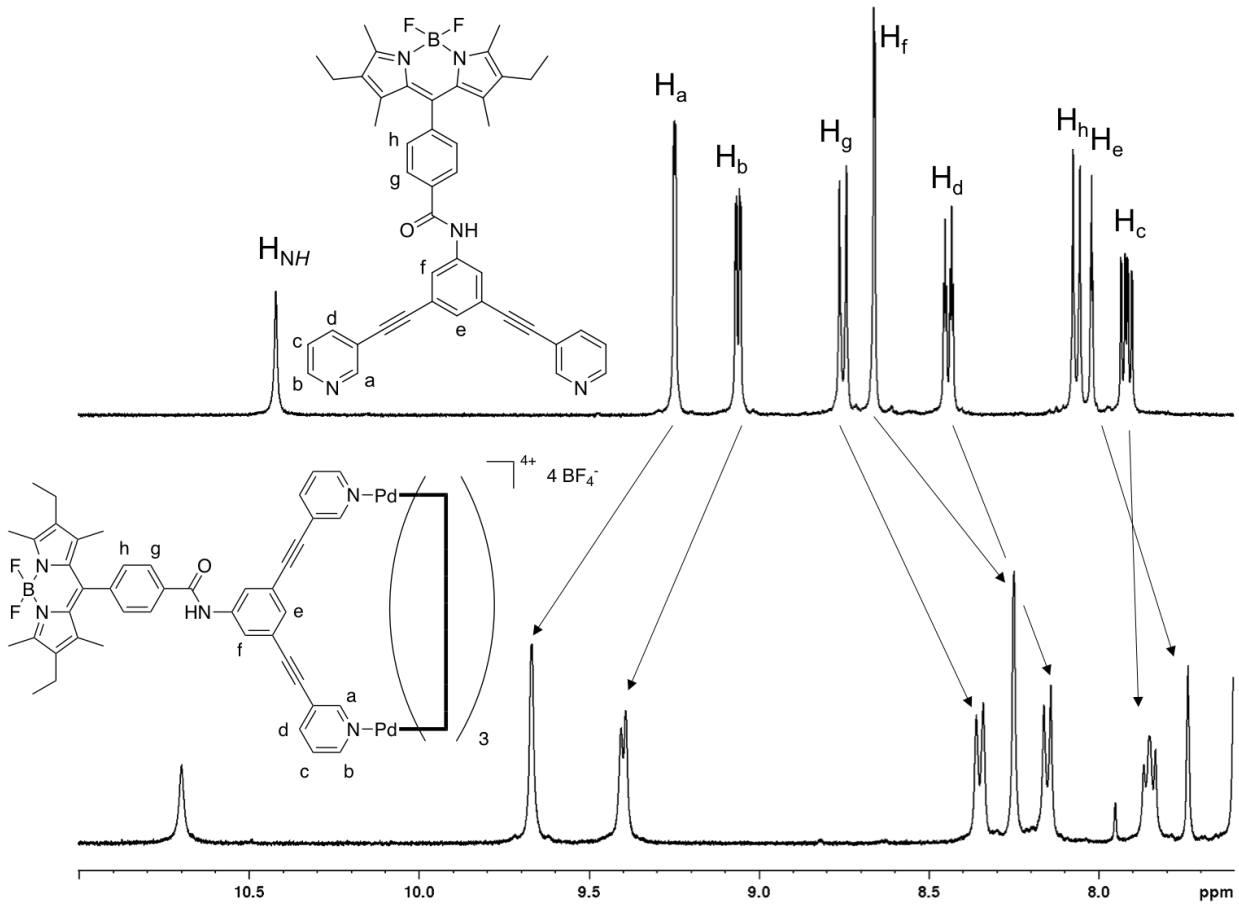

Figure 1 – Stacked ^{1}H NMR spectra zoomed into the aromatic region showing: Top: ligand **LB1** (DMSO-d_6). Bottom: Metallacage **C1.BF$_4$** (DMSO-d_6). Self-assembly of the metallacages could be followed by the large downfield shift of peaks H_a and H_b indicative of coordination to the Pd(II) ions.

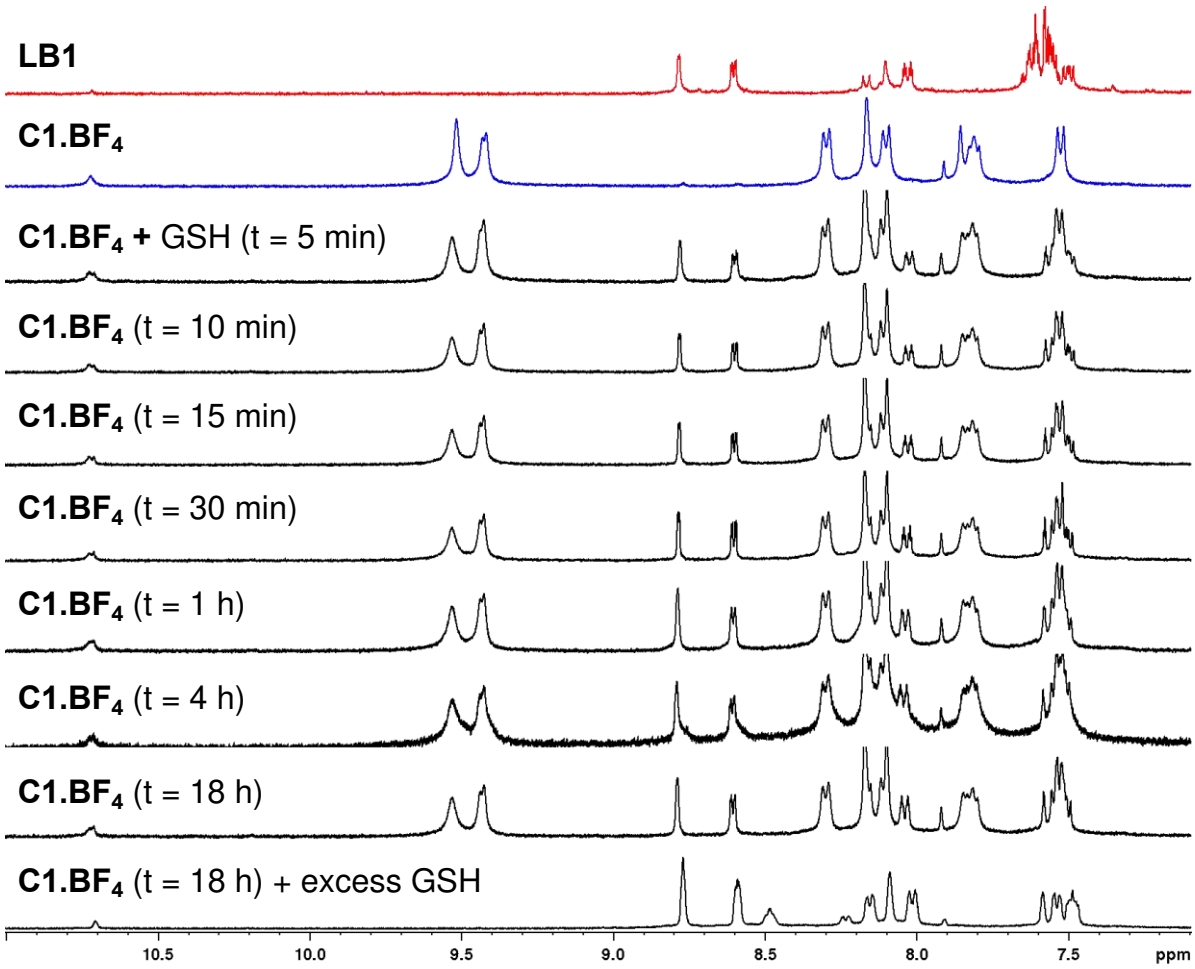

Figure 2. Stacked ^{1}H NMR spectra of ligand **LB1** (top) and of the corresponding metallacage **C1.BF$_4$** (second trace from top) in 9:1 ratio of DMSO-d_6: D_2O, in the presence of 2 mM glutathione over time. A further addition of excess GSH was performed after 18 h to achieve complete cage dissociation (bottom spectrum).

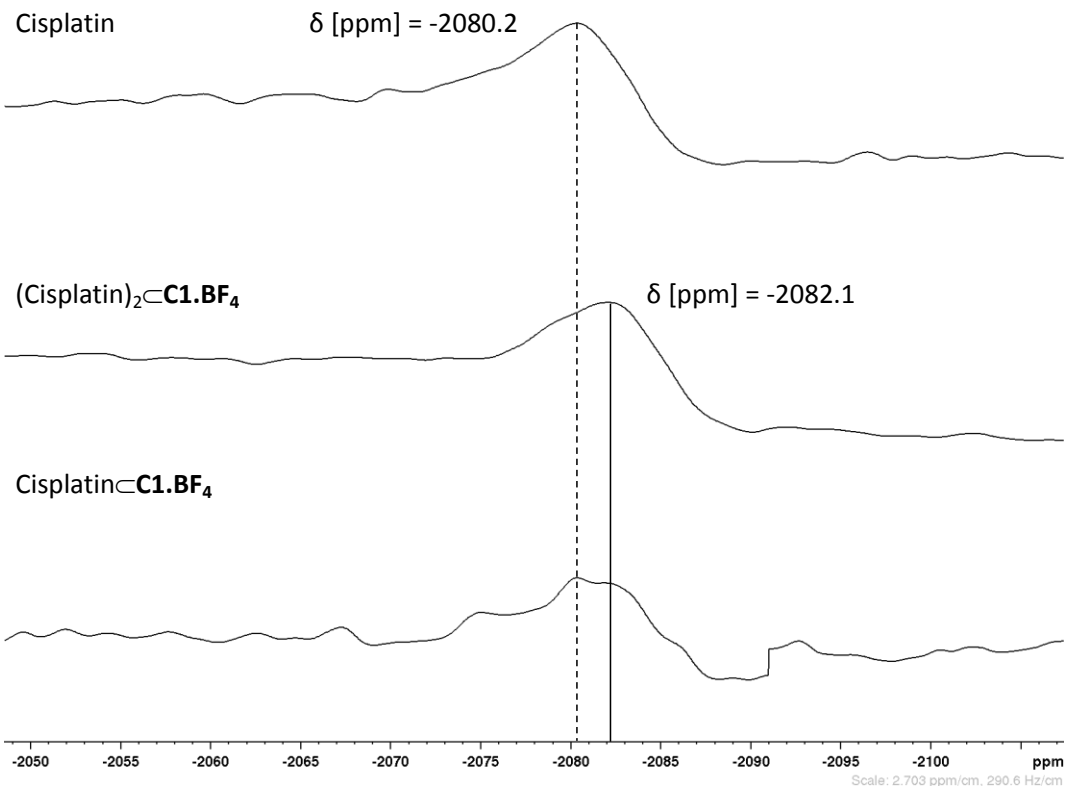

Figure 3 - Stacked ^{195}Pt NMR spectra in DMF of: (top) cisplatin (δ [ppm] = -2080.2); (middle) **C1.BF$_4$** + 2 equiv. of cisplatin (δ [ppm] = -2082.1); (bottom) **C1.BF$_4$** + 1 equiv. of cisplatin (δ [ppm] = -2082.1).

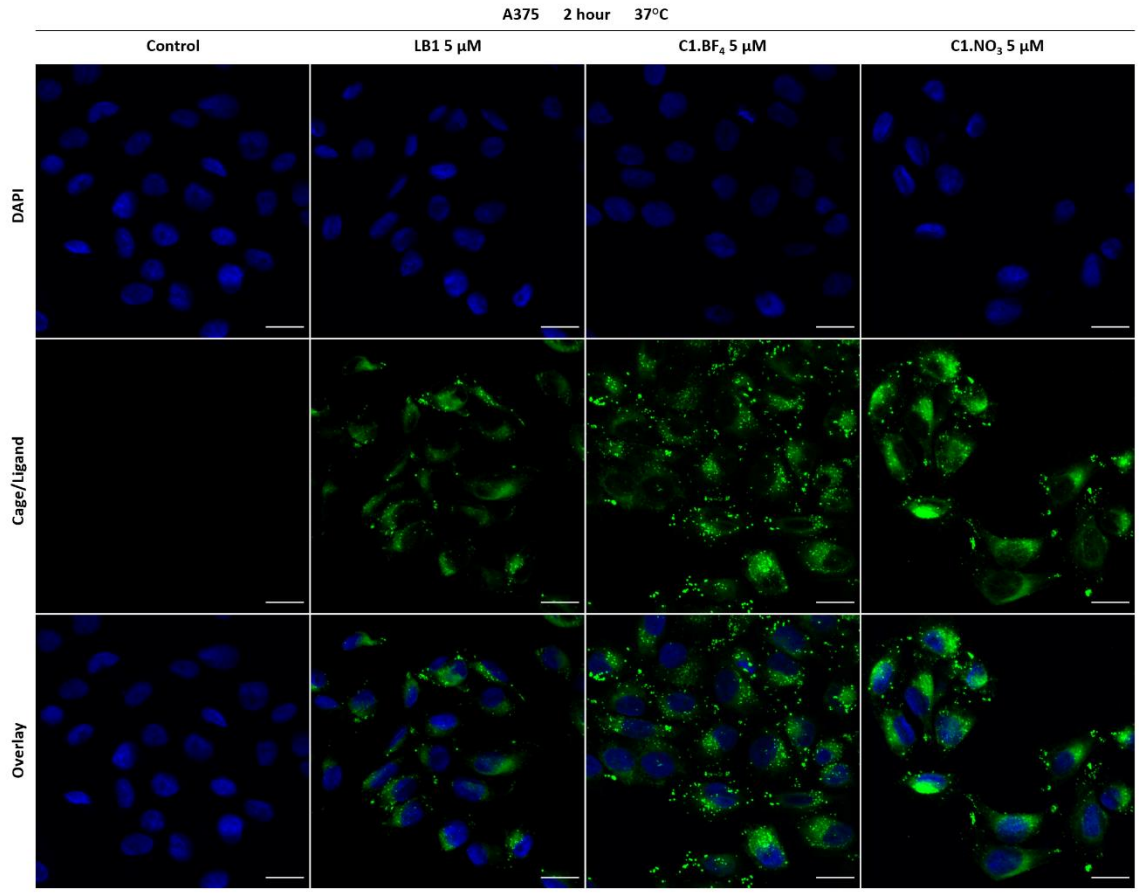

Figure 4 - Confocal Laser Scanning Microscopy (CLSM) Images of fixed human A375 melanoma cells pre-treated with ligand **LB1** or cages **C1.BF$_4$** and **C1.NO$_3$** for 2 h at 37 °C. Scale bar represents 20 µm. Data represents maximum projection images.

Table 1 - Photophysical data obtained by UV-Visible spectrophotometry and fluorescence spectroscopy for the BODIPY fluorophores (**B1** and **B2**), BODIPY functionalised bispyridyl ligands (**LB1** and **LB2**), and the fluorescent Pd_2L_4 metallacages (**C1.NO$_3$, C1.BF$_4$,** and **C2.NO$_3$**).

Compound	$\lambda_{max\ (Abs)}$ [nm]	ε_{max} [$M^{-1}\ cm^{-1}$]	$\lambda_{max\ (Em)}$ [nm]	ϕ_F [%]
B1	525	53 300	544	72
B2	525	72 700	543	75
LB1	290, 525	66 600	544	76
LB2	525	50 000	543	74
C1.NO$_3$	291, 527	42 100	544	50
C1.BF$_4$	291, 525	111 000	544	64
C2.NO$_3$	291, 525	160 000	543	70

Table 2 - Antiproliferative activity (EC_{50} values) of different cage and cage:cisplatin (1:2) formulations against human A375 cells after 24 h incubation, compared to cisplatin.

Compound	**EC_{50} (μM)[a]**
LB1	> 50
C1.NO$_3$	> 50
C1.BF$_4$	> 50
(cisplatin)$_2$⊂**C1.BF$_4$**[b]	29 ± 2
cisplatin	33.9 ± 2.9

[a] Data is presented as mean ± SEM of at least three independent experiments.
[b] The EC_{50} is calculated with respect to the concentration of free cisplatin.